Improved Understanding of Varestraint Testing—Nickel-Based Superalloys

Joel Andersson, Jonny Jacobsson, Anssi Brederholm and Hannu Hänninen

Abstract By Varestraint testing, the susceptibility of an alloy to hot cracking during welding can be evaluated on test plates when they are bent at the same time as welding takes place. The strains imposed by welding can thus be augmented by the strains imposed by the bending action to find the strain limits when hot cracks appear and also the sensitivity to hot cracking by counting the number and measuring the length of the individual cracks as a means to differentiate between the weldability of different alloys. Supports are usually recommended to avoid hinging and to use test plates thicker than 10 mm in order to minimize the influence of the compression strains (lower part of the bent specimen) on the weld cracking at the bending. The cracking response of two precipitation hardening Nickel-based superalloys—ATI 718Plus® and Haynes® 282®—was analysed in the context of the actual tensile/compression ratio imposed and measured by strain gauges attached to the upper and lower surface of the test plates. It was found that no influence of the compressive strains on the cracking response in Varestraint testing takes place. It was also seen that the hot cracking susceptibility of Haynes® 282® is lower compared to that of ATI 718Plus®.

J. Andersson (✉)
Department of Engineering Science, University West,
461 86 Trollhättan, Sweden
e-mail: joel.andersson@hv.se

J. Andersson · J. Jacobsson
GKN Aerospace Engine Systems, 461 81 Trollhättan, Sweden

J. Andersson · J. Jacobsson
Department of Materials and Manufacturing Technology,
Chalmers University of Technology, 412 96 Gothenburg, Sweden

A. Brederholm · H. Hänninen
Aalto University School of Engineering, Helsinki, Finland

Th. Boellinghaus et al. (eds.), *Cracking Phenomena in Welds IV*,
DOI 10.1007/978-3-319-28434-7_2

Varestraint Testing

Bending tests, such as the Varestraint testing, are among the most frequently used tests for evaluating the ductility of a metal or welded joint by measuring its ability to resist cracking during welding.

The Trans- and Varestraint tests, Fig. 1, are the two weldability testing methods that were developed by Savage and Lundin in the sixties [1] and are commonly employed when determining the weldability of a specific material. In the Trans-Varestraint testing method a weld is made transverse to the loading direction at the same time as a ram is pulling the plate downwards so that it is supposed to closely adhere to the mandrel located underneath the left-hand side of the plate. The die mandrel can be changed depending on what degree of strain one would like to achieve. Smaller radius gives higher strain. The crack length is then plotted as a function of strain. This testing method is primarily used for investigating the susceptibility towards solidification cracking.

The Varestraint testing which is primarily used for investigating heat affected zone (HAZ) cracking also addresses solidification cracking to some extent. The weld pass is performed in the longitudinal direction of the specimen as shown in Fig. 1.

Due to the heating from the welding torch, e.g. by GTAW, the material softens dramatically and a kink easily develops where the momentum is highest at the contact with the mandrel. The material does not fully adhere to the die located underneath the test material; as a consequence the material is not exposed to the intended ideal augmented strain, Fig. 2. When thin sheets are tested it is unfortunately not possible to avoid kinking as shown in the side view of Fig. 2. The material at the kink does not experience the expected amount of strain which therefore makes the results difficult to interpret.

To avoid kinking it is a common practice to use expendable support plates which force the test plate to ideally conform to the die mandrel since the effect of the soft spot due to the heating in the test material is reduced. However, these support plates do not impose tensile stresses in the test plates as schematically shown in Fig. 3, as bending is the process by which a straight length is transformed into a curved

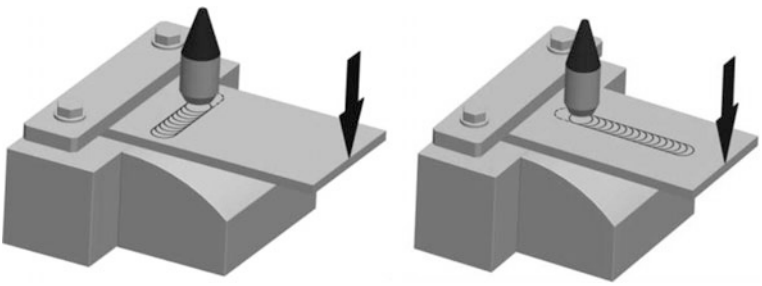

Fig. 1 Trans- and varestraint test, respectively

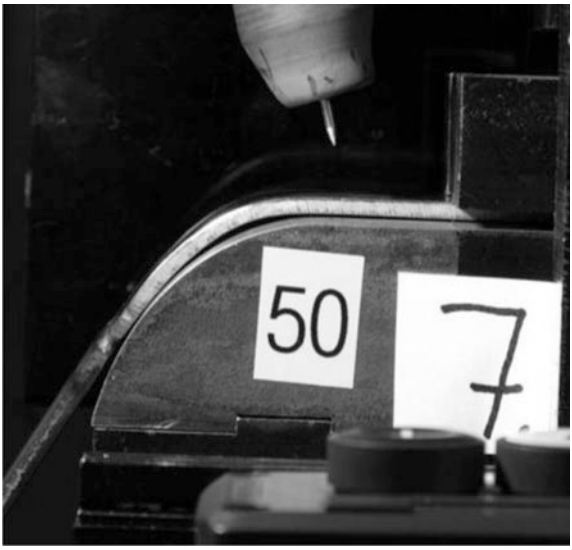

Fig. 2 Sideviews revealing how the testing plate kinks in varestraint testing

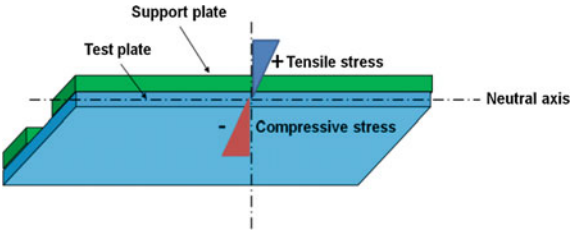

Fig. 3 Schematic sketch of a test plate with two support plates on top to avoid kinking in varestraint testing

length. The fibers of the metal on the outer (convex) surface of the bend are stretched, thus inducing tensile strains. Simultaneously, the fibers on the inner (concave) surface of the bend are exposed to compressive (negative) strains. Due to the physical nature of the bending tests both tensile (upper half of the plate) and compressive (lower half of the plate) stresses/strains are encountered during bending, Fig. 3.

This means that compressive stresses will develop within the weld in testing of sheet thicknesses below ~ 7 mm (assuming a weld depth of ~ 3 mm using GTA welding process). Thickness above ~ 7 mm is seldom used in aerospace applications and the value of Varestraint testing may be limited in this context and this limitation is addressed in the present study. The aim of the present study is to investigate how the state of stress/strain affects the cracking response in Varestraint testing.

Varestraint Testing of Precipitation Hardening Nickel-Based Superalloys

ATI 718Plus® and Haynes® 282® are two newly developed precipitation hardening Nickel-based superalloys with promising characteristics. Both alloys benefit from the gamma prime phase which provides high temperature strength up to 704 and 800 °C, respectively [2–4]. Welding of the precipitation hardening Ni-based superalloys is of great importance in the manufacturing of structural components used for aero engines [5]. It is therefore necessary to investigate how these alloys behave and respond to different welding operations. One tool is the Varestraint testing to investigate on a more fundamental level how the alloys perform in terms of weldability. There is very limited amount of Varestraint studies for these two alloys. However, previous Varestraint studies performed [5] on ATI 718Plus® indicate that hot cracking resistance seems to be at par with Alloy 718. Hot cracking resistance was associated with Nb-rich MC and Laves phase constituents. No Varestraint studies have been published on Haynes® 282® but Gleeble test results [5] indicate that Haynes® 282® possesses good hot ductility. Liquation was associated with different types of MC.

Experimental

Varestraint Testing

Two different Varestraint testing configurations, Fig. 4, were used to investigate how the tensile/compressive stress ratio influences the cracking response in testing. The configuration on the left-hand side has the tack-welded support plates on the bottom side of the test plates whereas the configuration on the right-hand side (the normal way) has the support plates lying free on top of the test plate.

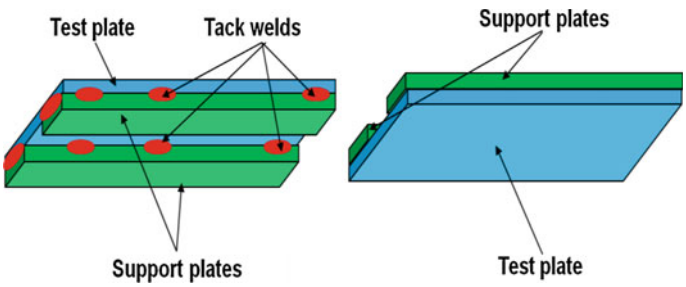

Fig. 4 Varestraint testing configurations in the present study

Table 1 Test parameters at bending without welding

Material	Test plate thickness (mm)	Support plate thickness (mm)
304 stainless steel	2	6
304 stainless steel	3	5
304 stainless steel	5	3

Table 2 Test parameters in standard varestraint testing

Material	Test plate thickness (mm)	Support plate thickness (mm)	Welding parameters	Stroke rate (mm/s)
ATI 718Plus® and Haynes® 282®	3.2	5	TIG welding source, 85 A current and 2 mm/s welding speed	15

The configuration on the left-hand side will only impose tensile stresses in the test plate upon bending while the right-hand side configuration will impose both tensile and compressive stresses upon bending.

Strain gauges were used on top and bottom side of the test plates (both configurations) in pure bending (without welding) to verify what was assumed regarding the tensile/compressive stress ratio.

The actual testing parameters in pure bending and Varestraint testing are shown in Tables 1 and 2, respectively.

Material

Expendable AISI 304 stainless steel with different thicknesses (Table 2) was used in the bending experiments to investigate the tensile and compressive stress ratio. The materials used in Varestraint testing were in the mill-annealed condition with an average Vickers hardness (1 kg load) of HV 330 (ATI 718Plus®) and HV 215 (Haynes® 282®). The grain size (GS) of ATI 718Plus® and Haynes® 282® was 10 and 65 µm, respectively (Fig. 5).

The chemical compositions (wt%) are shown in Table 3.

Metallographic Procedures

Scanning electron microscopy (SEM) and energy dispersive X-ray spectroscopy (EDS) was used on samples ground, polished and etched (electrolytically with oxalic acid at 2–5 V for 3–10 s) according to common practice. Fluorescence penetrant inspection together with digital imaging software was used to evaluate the amount of cracking at Varestraint testing.

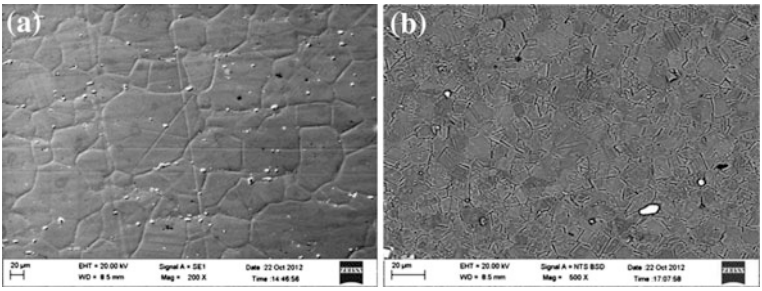

Fig. 5 The microstructure of as-received material: **a** Haynes® 282® (GS 65 μm, HV 215) and **b** ATI 718Plus® (GS 10 μm, HV 330)

Table 3 Chemical compositions in wt% of ATI 718Plus® and Haynes® 282®

Element	ATI 718Plus®	Haynes® 282®
Ni	Bal.	Bal.
Cr	18.0	19.63
Fe	9.6	0.35
Co	8.9	10.35
Mo	2.6	8.56
Al	1.52	1.41
Ti	0.74	2.21
Nb	5.47	–
C	0.02	0.068
P	0.010	0.002
B	0.005	0.004
Mn	0.12	0.08
S	0.0003	0.002
Si	0.08	–
W	1.0	–

Results and Discussion

Strain Measurement

The strain measurements in pure bending of the test plate without tack-welded support plates are shown in Fig. 6. Here, the target strain was calculated according to Eq. 1 below and estimated to ~ 2 %.

$$\varepsilon = t/2R \tag{1}$$

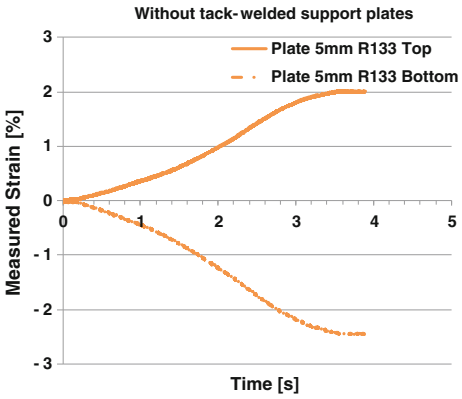

Fig. 6 Example of strain measurement in pure bending with a target strain of ~2 % using a test plate thickness of 5 mm and radius of 133 mm (R133) with support plates lying free on top of the test plate. The *solid line* reveals measurements from the *top side* of the test plate, whereas the *dotted line* represents measurements from the *bottom side* of the same test plate

where
t = thickness of the plate (mm)
R = the size of the radius die mandrel (mm)

It is clearly revealed that the upper half of the plate thickness is in tension (about 2 %) whereas the lower half is exposed to compressive strains (about −2 %) in bending.

The bending tests with tack-welded support plates are shown in Fig. 7. A constant total thickness of 8 mm (support plate plus test plate) was used throughout the testing. A smaller test plate thickness was thus compensated by a larger tack-welded support plate thickness. So, while decreasing the test plate thickness and increasing the thickness of the tack-welded support plates, the compressive strains imposed upon bending will decrease. In fact, support plates of 6 mm and a testing plate of 2 mm is the only case which reveals any compressive strains in bending. This means that the following target strains were aimed for:

- Sample 1–2: (top surface), 2 %—(bottom surface), −0.25 %
- Sample 3–4: (top surface), 2 %—(bottom surface), 0.25 %
- Sample 5–6: (top surface), 2 %—(bottom surface), 0.5 %

All the target strains coincide fairly well with the results presented in Fig. 7 except the bottom side of the sample 5–6 (~1 % on the bottom side) which seems to exceed the estimated target strain of 0.5 %. The reason for this is not clear but could be associated with lack of fixturing and/or error in the mounting of strain gauge.

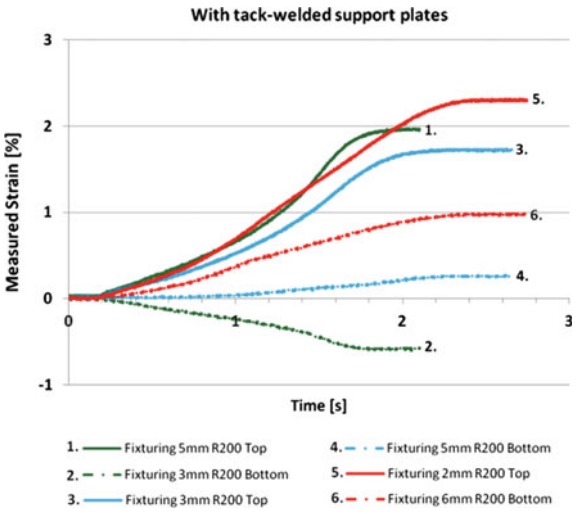

Fig. 7 Strain measurement in pure bending using a radius of 200 mm (R200) with tack-welded support plates on the *bottom side* of the test plate. The *solid lines* are measurements from the *top side* of the test plates, whereas the *dotted lines* with the same colour are measurements from the bottom side of the same test plate (color figure online)

Varestraint Testing of ATI 718Plus® and Haynes® 282®

The total crack length (TCL) response versus ideal augmented strain of ATI 718Plus® and Haynes® 282® in Varestraint testing using both test configurations (that is with and without tack-welded support plates) is shown in Figs. 8 and 9, respectively. Surprisingly, no distinction between the different plate configurations could be made in Varestraint testing of ATI 718Plus® and Haynes® 282® despite the presumably different strain situations within the materials. There is certainly a difference in state of strain in Varestraint testing compared to pure bending where no weld fixturing interferes. The exact strain situation when welding influences to

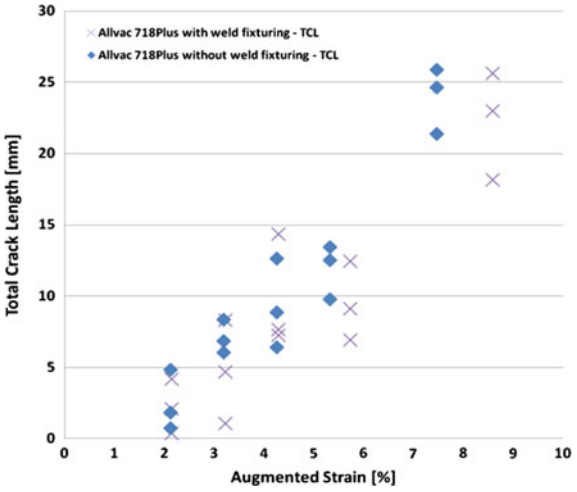

Fig. 8 The crack response in terms of TCL of ATI 718Plus® in varestraint testing using both test configurations

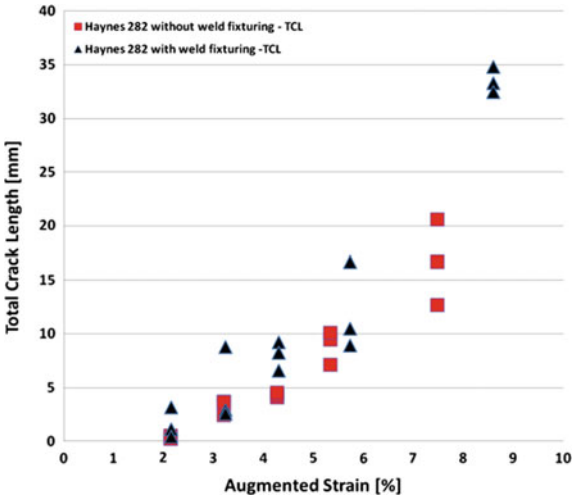

Fig. 9 The crack response of Haynes® 282® in varestraint testing using both test configurations

the bending process is complex and difficult to visualize. Another fact is that in the evaluation of the Varestraint test materials, only cracks visible on the surface are considered and not the cracks underneath the surface. Since only surface cracks are measured and both test configurations are exposed to the same magnitude of strain at the top surface, it seems that whatever state of strain under the surface it does not influence the cracking response at the surface. Thus, it does not matter if the lower half of the test plate is exposed to compressive strains and very thin plates can consequently be tested as long as support plates are used to avoid kinking.

Hot cracking (FZ and HAZ) results for both Haynes® 282® and ATI 718Plus®, as shown in Fig. 10, indicate comparable susceptibility to hot cracking. Remembering the positive effect of small grain size on weldability and the large difference in grain size, ASTM 5 for Haynes® 282® and the very fine ASTM 10 grain size for ATI 718Plus®, it can definitely be expected that Haynes® 282® possesses a better hot cracking resistance compared to that of ATI 718Plus®.

Looking closer into the weld microstructure and especially the liquated grain boundaries within the HAZ of ATI 718Plus®, Fig. 11, it appears as if NbC has experienced constitutional liquation.

The constitutional liquation of NbC is supported and validated by the elemental phase map presented in Fig. 12 which indicates the presence of NbC and Laves phase. It should be noted that it is not possible to quantify C using SEM-EDS analysis, but the C-levels between the matrix phase and the NbC/Laves constituents are different indicating the presence of C in the first one. Both of these two phases (NbC and Laves) contain large amount of Nb [5]. As temperature increases rapidly and as the MC is in contact with the γ-matrix a local equilibrium promotes the transformation to γ-Laves mixture due to the constitutional liquation.

Haynes® 282® on the other hand did not reveal significant liquation in the HAZ as ATI 718Plus®, Fig. 13. However, in SEM examination of the HAZ it is seen that

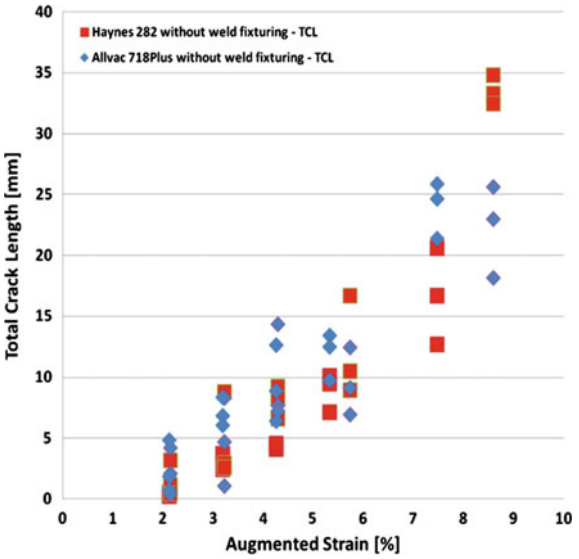

Fig. 10 Comparison in cracking response between Haynes® 282® and ATI 718Plus® in varestraint testing using both test configurations

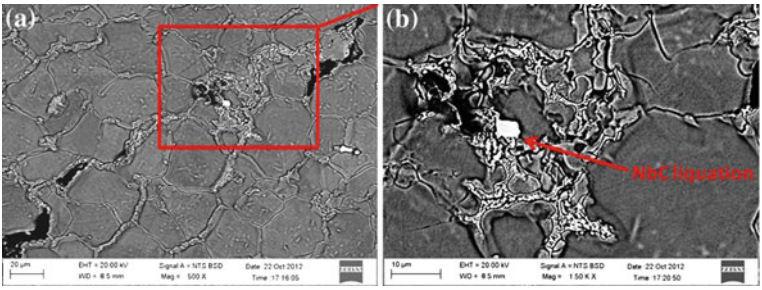

Fig. 11 Constitutional liquation of NbC in ATI 718Plus®

also in this alloy constitutional liquation of MC takes place locally due to the rapid heating, see Fig. 13.

The MC liquation in Fig. 13 does reveal enrichment of Mo, C and S, as seen in Fig. 14, indicating the presence of MoC [6]. However, care should be taken with the indication of S since the Mo and S energy peaks overlap and may result in an erroneous interpretation of the results.

The situation is complex, since many elements are involved and a non-equilibrium situation is encountered due to the fast heating and cooling. However, it is possible that a ternary interaction between Mo(C) and Ni-S occurs. It is well known that Ni-S and Ni-Mo have eutectic transformations at ~600 and 1315 °C, respectively [7–9]. It is not unreasonable that a ternary eutectic may be

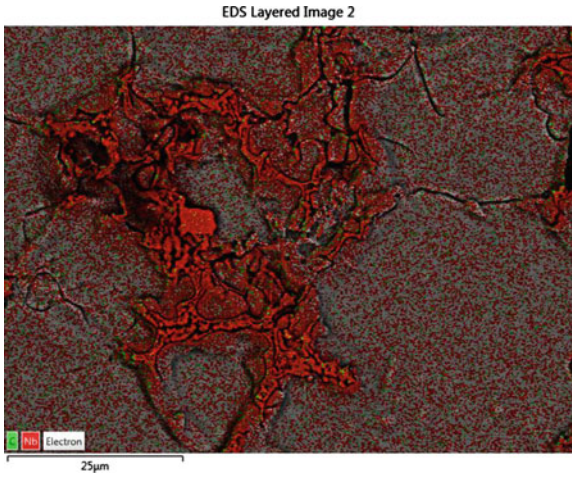

Fig. 12 SEM-EDS elemental map of ATI 718Plus® revealing enrichment of Nb and C

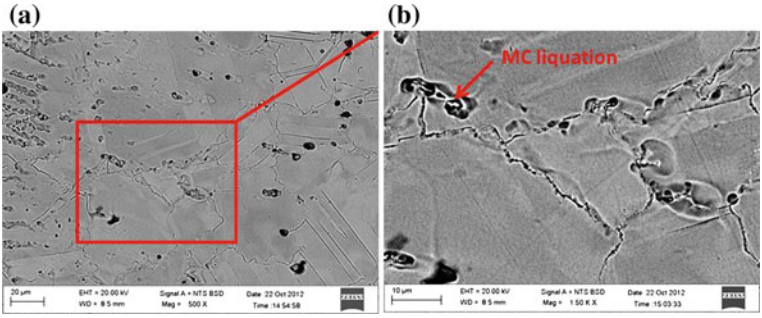

Fig. 13 Constitutional liquation of MC in Haynes® 282®

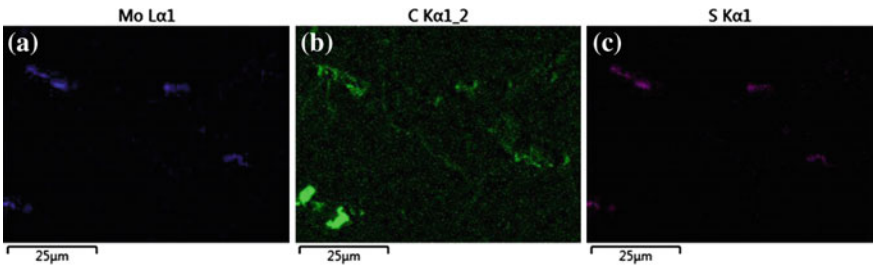

Fig. 14 SEM-EDS elemental maps of a liquated grain boundary in Haynes® 282® revealing enrichment of **a** Mo, **b** C and **c** S

present due to the non- equilibrium diffusion of S and causing the liquation in Haynes® 282®. Since only traces of S are present in the two alloys of our study the non- equilibrium diffusion of S offers an explanation, but this is still to be verified by the use of more sophisticated analysis tools.

Conclusions

1. No influence of the compressive strains on the cracking response in Varestraint testing was observed.
2. Thin test plates can be used as long as kinking is eliminated when support plates are used.
3. Hot cracking susceptibility of Haynes® 282® is lower compared to that of ATI 718Plus® especially when the grain size effects are considered.
4. ATI 718Plus® liquates through constitutional liquation of NbC.
5. A hypothesis regarding liquation of MoC through eutectic transformation of Ni-Mo or Ni-Mo-S in Haynes® 282® is possible.

Acknowledgements We thank Mr. Heikki Vestman at Aalto University School of Engineering for his help with Varestraint testing. We also thank Professor Lars-Erik Svensson and Leif Karlsson at University West as well as Dr. Göran Sjöberg at GKN Aerospace Engine Systems Sweden for fruitful input and guidance.

References

1. Savage W. F., and Lundin C.D.; “The Varestraint Test”, The Welding Journal, October, 1965, pp. 433- 442.
2. Cao W.D.; “Nickel-Base Alloy”, U.S. Patent 6,730,264 B2, May 04, 2004.
3. Kennedy R. L.; ”Allvac 718Plus, Superalloy for The Next Forty Years”, Superalloys 718, 625, 706 and Various Derivatives, TMS, Warrendale, PA, 2005, pp. 1-14.
4. Pike L. M.; ”Development of a Fabricable Gamma – Prime (γ’) Strengthened Superalloy”, Superalloys 2008, eds. R.C. Reed, K.A. Green, P. Caron, T. P. Gabb, M. G. Fahrmann, E. S. Huron, S. A. Woodard, The Minerals, Metals & Materials Society, 2008, pp. 191-200.
5. Andersson J.; “Weldability of Precipitation Hardening Superalloys – Influence of Microstructure”, PhD Thesis, Chalmers University of Technology, Gothenburg, Sweden, 2011.
6. Osoba, L.O., Ding, R.G., and Ojo, O.A.; “Microstructural Analysis of Laser Weld Fusion Zone in Haynes 282 Superalloy”, Materials Characterization, 65 (7), 2012, pp. 93.
7. Hansen M., and Anderko K.; “Constitution of Binary Alloys”, McGraw-Hill, 1958.
8. R.P. Elliot, “Constitution of Binary Alloys”, First Supplement, McGraw-Hill, 1965, pp. 968.
9. Okamoto H.; “Ni-S (Nickel-Sulfur)”, Journal of Phase Equilibria andDiffusion, 30 (1), 2009, pp. 123.

http://www.springer.com/978-3-319-28432-3

Cracking Phenomena in Welds IV
Boellinghaus, Th.; Lippold, J.C.; Cross, C.E. (Eds.)
2016, XI, 512 p. 358 illus., Hardcover
ISBN: 978-3-319-28432-3